LETTERS IN HEAT AND MASS TRANSFER 0094-4548/78/0501-0151$02.00/0
Vol. 5, pp. 151 - 166, 1978

MECHANICS OF DROPLET EVAPORATION ON HEATED SURFACES

Wen-Jei Yang
Department of Mechanical Engineering
The University of Michigan
Ann Arbor, Michigan 48109

(Communicated by J.P. Hartnett and W.J. Minkowycz)

ABSTRACT

This paper examines the mechanics of evaporation of liquid droplets in direct contact with heated surfaces whose temperature is below the maximum boiling-rate point. The study leads to a classification of the evaporation mode into three categories (i) where the evaporation is controlled by heat transfer through the droplet, (ii) where conduction in the heating plate is the controlling mechanism, and (iii) the intermediate case, where both effects are of comparable importance. A dimensionless parameter is identified which may be employed to characterize the mode of evaporation. Experimental results indicate the general validity of the theoretical analysis.

Introduction

A typical droplet lifetime curve, a plot of lifetime t_ℓ versus the surface temperature T_w, takes the form of an inverted boiling curve, Fig. 1. When T_w is below the liquid boiling point T_b, liquid drops spread into a thin layer and evaporate slowly. This range a-b is called the "liquid-film" type evaporation regime in which the heat is transferred from the surface to the liquid by convection. At the point b when T_w is equal to the liquid boiling point, nucleate boiling is observed in the spreading drop. When the maximum boiling rate is reached at point c, the liquid forms a spherical drop which intermittently makes contact with the surface and vaporizes violently. The range b-c is referred to as the "nucleate-boiling" type vaporization regime. The Leidenfrost point d indicates the interruption of contact between the drop and the heating surface due to the formation of a stable vapor film. With T_w beyond the point d, the liquid is evaporated from the heating surface by a stable layer of vapor. The ranges c-d and d-e are called the transition and spheroidal (i.e., film boiling) vaporization regimes, respec-

tively. It is only within the ranges a-b and b-c that a liquid droplet is in direct contact with the heating surface during its evaporation process.

The evaporation of a droplet in direct contact with a heated surface may be viewed as a problem of determining the rate of unsteady heat transfer from the heating plate to the droplet surface (gas-liquid interface) where evaporation takes place. The rate depends not only on the internal resistance within the droplet and the droplet surface-to-ambient resistance but also on non-uniformity in plate temperature. The latter can be explicitly related to the thermal conductivity and heat capacity of the plate material. Initially, the plate is maintained at a uniform temperature T_w. When a drop is placed on it, the local plate temperature changes with time as a result of heat transfer to the drop across the liquid-solid interface. The local surface temperature remains at T_w only if the plate material has an infinite thermal conductivity and heat capacity. For any surface with a finite thermal conductivity and heat capacity, the local temperature is dependent on the local heat flux. Hence, there is coupling between the momentum and energy equations in the liquid and the equation for the temperature field in the solid and the general problem becomes quite complex.

Perhaps the earliest work of drops resting on horizontal surfaces (sessile drops) was due to Bashforth and Adams [1]. After developing a method of calculating by quadratures the exact theoretical forms of drops of fluids from the differential equation of Laplace, Bashforth in 1857 calculated droplet forms and determined the effects of physical properties and surface temperature on droplet shapes. Savic and Boult [2] presented a theory of the fluid flow associated with the impact of liquid drops with a solid surface. The shape of the spreading drop was calculated as well as the pressure distribution over the impact plane. It was found in references 1 and 2 that both the sessile and impinging drops are lens(dome)-shaped on horizontal surfaces. Experimental observations confirmed the prediction.

Tamura and Tanasawa [3] measured the lifetime of impinging drops of various liquids on a heated quartz plate with surface temperatures ranging from below the boiling point to over the ignition point of the liquids. Although they observed a sudden fall in surface temperature when the droplet made contact with the surface, the surface temperature was assumed constant at its initial value T_w in data correlations. The solid conduction was thus neglected and the evaporation was presumed to be controlled by the rate of

heat transfer through the droplet. Teshirogi [4] suggested an importance of heat conduction in the heating plate to the evaporation rate. He used the specific heat capacity of the solid as a parameter to correlate test data for the evaporation of impinging drops of various liquids on three heating plates of different materials. As will be pointed out later in the Discussion section, solid conduction effects in his case were entirely negligible and the evaporation was controlled by heat transfer through the droplet. Both references 3 and 4 reported that those evaporating drops in the "liquid-film" and "nucleate-boiling" evaporation regimes were lens-shaped.

Theory [5] was developed on the evaporation of sessile and impinging drops on heated surfaces for the evaporation mode controlled by heat transfer through the droplets. The study was extended to the case of binary liquid drops in reference 6. Results of both pure and binary liquid drops agreed well with test data of references 3 and 4. Numerous works have been reported on the droplet evaporation in the spheroidal vaporization regime. Since a droplet evaporating in the spheroidal regime is not in direct contact with the heating surface, a review on these works is not presented here.

Bascom et al [7] investigated the mechanisms of spontaneous spreading of liquid drops over unheated horizontal and vertical surfaces. It is disclosed that the spontaneous spreading of liquids on smooth, clean metal surfaces is characterized by the advance from the bulk liquid of an invisible primary film less than 1000 A. thick, usually followed by a visible thicker secondary film. The primary film is considered to advance largely by surface diffusion, while the movement of the secondary film results from a surface tension gradient, i.e. Marangoni effects, across the transition zone between the primary and secondary films. This gradient is produced by the unequal evaporation depletion from these two regions of a volatile contaminant having a lower surface tension. If the volatile contaminant has a higher surface tension than the main components, the gradient is reversed and the liquid recedes. Removal of the volatile constituents eliminates the secondary but not the primary spreading. Liquid may also spread by capillary flow in microscratches. The drop initially assumes a lens-shaped profile. As the liquid film advances on the surface, it develops a plateau region with a leading edge at a small angle to the solid surface. (This will not be observed on a heated surface, for which the drop will maintain a lens-shaped profile during evaporation process.) Progressively, a ridge is developed

behind the edge, still maintaining an apparent contact angle with the solid. Molecules having highly polar functional groups are generally adsorbed on metal surfaces to form monomolecular films over which the liquid cannot spread. On the other hand, relatively low polar liquids will spread with an apparent angle of contact.

While the effect of heat transfer through drops on evaporation is well documented, that of plate conduction has not yet been explored. Thus, it appears that there is a definite need to establish conditions under which either effect or both are important in controlling evaporation rate. This paper examines the relative importance of these two effects for liquid drops evaporating on heated surfaces. The problem is first formulated generally, followed by simplifications to a form that is tractable to a solution. The analysis leads to a classification of the evaporation mode into three categories. A dimensionless parameter is identified to characterize the mode of evaporation. The theoretical analysis is compared with experimental results [3,4].

Analysis

Formulation of the problem on drop evaporation is much simplified if a hemispherical geometry is considered, Fig. 2-a. However, analysis may be readily extended to the general case in which the drop geometry is a spherical segment with a contact angle θ, Fig. 2-b. The former geometry is employed for demonstrating the formulation in the interest of brevity, since a closed-form analytical solution for either case is apparently not obtainable. Transport of sensible heat from the drop to the ambient at T_a is assumed negligible compared to the transfer of latent heat as a result of evaporation. An equivalent heat transfer coefficient h_a is defined at the liquid-ambient interface. Two limiting conditions for heat transfer through the drop are treated: conduction-controlling and rapid mixing mechanisms.

1. Conduction-controlling model

In this model, internal fluid motion does not exist such that diffusion is the only heat transfer mechanism. This represents the slowest internal heat transfer limit. The conduction equation for the droplet in spherical coordinates (ζ, ϕ) reads

$$\frac{1}{a'}\frac{\partial T'}{\partial t} = \frac{1}{\zeta^2}\frac{\partial}{\partial \zeta}\left(\zeta^2 \frac{\partial T'}{\partial \zeta}\right) + \frac{1}{\sin\phi}\frac{\partial}{\partial \phi}\left(\sin\sigma \frac{\partial T'}{\partial \phi}\right)$$

The initial and boundary conditions are

$$T'(\zeta,\phi,0) = T'_o$$

$$T'(\zeta, \pm\pi/2,t) = T(r,o,t) \text{ ---- for } 0<\zeta<R \text{ and } r = \zeta$$

$$T'(0,\phi,t) = \text{finite}$$

$$\partial T'(R,\phi,t)/\partial\rho = (h_a/k')[T_a - T'(R,\phi,t)]$$

Here, T denotes the temperature; a, thermal diffusivity; t, time; T_o, initial droplet temperature; R, instantaneous droplet radius; k, the thermal conductivity; and '(superscript), liquid phase (droplet).

Cylindrical coordinates (r,z) are used for the surface. The energy equation is

$$\frac{1}{a}\frac{\partial T}{\partial t} = \frac{1}{r}\frac{\partial}{\partial r}\left(r\frac{\partial T}{\partial r}\right) + \frac{\partial^2 T}{\partial z^2}$$

subject to the initial and boundary conditions

$$T(r,z,o) = T_w$$

$$\partial T(o,z,t)/\partial r = 0$$

$$k\partial T(r,o,t)/\partial z = k'\partial T'(\zeta, \pm\pi/2,t)/\partial z$$
$$\ldots \text{ for } 0<\zeta<R \text{ and } r = \rho$$

$$k\partial T(r,o,t)/\partial z = h_a[T(r,o,t)-T_a]$$
$$\ldots \text{ for } R<r<\infty$$

$$T(\infty,z,t) = T_w$$

$$T(r,\infty,t) = T_w$$

A finite element (or difference) computer program of good scale will be required for a solution of the two sets of coupled equations. In order to gain some insight into the mechanism and to determine the effects of the governing dimensionless parameters, the problem will be simplified as follows: The response of the liquid temperature is much slower than that of the surface temperature because of very low liquid thermal diffusivity. Since droplet lifetime is short, generally in seconds, it is appropriate under the condition of drop evaporation to deal with only the heating-surface temperature variation. The contribution of heat transfer through the droplet is compensated as a thermal resistance. In other words, the flow of heat from the heating surface to the ambient is controlled by two resistances, namely

the conductive resistance through the droplet and the liquid-ambient interfacial resistance $1/(2\pi R^2 h_a)$.

In a study on dropwise condensation, Umur and Griffith [8] have solved the steady-state phase of the droplet equations, treating the liquid-solid interfacial temperature as T_w. They obtained an expression for the heat transfer rate through the drop. Subsequently, Mikic [9] has imposed a simplification on the expression through the use of an equivalent conductive resistance $1/(4\pi k'R)$. If h_d is the conductive heat transfer coefficient in the droplet, one can write $h_d = 4k'/R$.

Another simplification is to consider heat conduction in the heating plate as one-dimensional in the z direction. The governing equations can be written as

$$\partial T/\partial t = a\partial^2 T/\partial z^2 \tag{1}$$

$$T(z,o) = T_w \tag{2}$$

$$T(\infty,t) = T_w \tag{3}$$

$$k\partial T(o,t)/\partial z = U[T(o,t)-T_a] \tag{4}$$

Here, the overall heat transfer coefficient between the surface and the ambient based on the liquid-solid interfacial area U is defined as

$$1/U = 1/(2h_a) + 1/h_d \tag{5-a}$$

in which

$$h_d = 4k'/R_o \tag{6-a}$$

and $h_a = k_a/R_o$ is derived from Nu = 2 for natural convection over a spherical droplet. Nu represents the Nusselt number and k_a is the thermal conductivity of the ambient gas. Both heat transfer coefficients h_d and h_a are evaluated on the basis of the initial droplet size R_o.

The solution of equations (1) through (4) are obtained in non-dimensional form as

$$[T(Z,X)-T_a]/\Delta T = \text{erf } Z + \exp(2ZX + X^2)\text{erfc}(Z + X) \tag{7}$$

in which

$$\Delta T = T_s - T_a,\ Z = z/[2(at)^{1/2}],\ X = (U/k)(at)^{1/2} \tag{8}$$

With the aid of equation (7), the heat flux across the liquid-solid interface is found to be

$$q_b = -4\pi R^2 \psi_b U \Delta T \exp X^2 \operatorname{erfc} X \tag{9}$$

Now, consider a droplet of lens-shaped profile. Its idealized geometry, as shown in Fig. 2-b, consists of a spherical segment with contact angle θ. Its base area, surface area and volume are $4\pi R^2\psi_b$, $4\pi R^2\psi_s$ and $4\pi R^3\psi_v/3$, respectively wherein

$$\psi_b = \sin^2\theta/4, \quad \psi_s = (1-\cos\theta)/2, \quad \psi_v = [2-\cos\theta(2+\sin^2\theta)]/4 \tag{10}$$

The total heat transferred to a drop of radius R may be expressed as

$$Q = \rho' \lambda 4\pi R^3 \psi_v/3 \tag{11}$$

where ρ and λ denote the density and latent heat of vaporization, respectively. The heat balance on the drop reads $dQ/dt = q_b$. With the aid of equations (9) and (11), one obtains

$$\rho' \lambda \psi_v dR/dt = -U\Delta T \psi_b \exp X^2 \operatorname{erfc} X \tag{12}$$

Since the drop geometry is generalized from a hemisphere to a spherical segment, both U and h_d must be geometrically modified as

$$1/U = \psi_b/(\psi_s h_a) + 1/h_a \tag{5-b}$$

and

$$h_d = k'/(\psi_b R_o) \tag{6-b}$$

respectively. Equation (12) is integrated subject to the initial condition $R(o) = R_o$. One obtains

$$R/R_o = 1 - \phi(\tau)/Y \tag{13}$$

wherein

$$Y = \psi^* \rho' \lambda U R_o/K\Delta T, \quad \psi^* = \psi_v/\psi_b \tag{14}$$

$$\phi(\tau) = \int_o^\tau \exp y \operatorname{erfc} y^{1/2} dy \tag{15}$$

$$\tau = X^2 = U^2 t/K, \quad K = \rho C k \tag{16}$$

The droplet lifetime t_ℓ may be obtained from equation (13), corresponding to $R = 0$, as

$$\phi(\tau^*) = Y \tag{17}$$

in which

$$\tau^* = U^2 t_\ell/K \tag{18}$$

2. Lumped-parameter (rapid-mixing) model

In this model, internal fluid motion induces very rapid convective heat transfer such that h_d becomes infinite. Therefore, the overall heat transfer coefficient is deduced to

$$U = \psi_s k_a/(\psi_b R_o) \tag{5-c}$$

This model represents the fastest internal heat transfer limit. All equations (7) through (18) still apply. A comparison of equations (5-b) and (5-c) reveals that U for the lumped-parameter model is larger than U for the conduction-controlling case.

Results and Discussion

The quantity $t_c = K/U^2$ in the definition of the dimensionless times τ and τ^* represents the characteristic time which defines the range of three different evaporation mechanisms, as will be discussed later in the section. Hence, it can be regarded as the time constant of the evaporating system. Equation (15) was numerically integrated using the trapezoidal rule. Results are graphically illustrated in Fig. 3. Two asymptotic expressions are obtained for $\phi(\tau)$:

For small values of τ, both the exponential and complimentary error functions may be expanded into infinite series [10]. One can then integrate equation (15) to give

$$\phi(\tau) = \sum_{n=1}^{\infty} \frac{\tau^n}{n!} - \frac{2}{\pi} \sum_{n=1}^{\infty} \frac{2^n \tau^{(2n+1)/2}}{(2n+1) \prod_{m=1}^{n} (2n+1-2m)}$$

When τ is less than 0.001, or equivalently $t^* < 0.001$,

$$\phi(\tau) = \tau \tag{19}$$

where t^* is defined as t_ℓ/t_c. A combination of equations (14), (17), (18) and (19) produces

$$t_{\ell 1} = \psi^* (\rho' \lambda/\Delta T)(R_o/U) = 3Q_o/q_{bo} \tag{20}$$

where $t_{\ell 1}$ denotes the droplet lifetime within this range of t^*. Q_o and q_{bo} correspond respectively to Q and $|q_b|$ at zero time when $R = R_o$.

Similarly, for large values of τ, the integrand of equation (15) may be approximated [10], followed by an integration to yield

$$\phi(\tau) \cong \frac{1}{\pi^{1/2}} \left(2\tau^{1/2} + \frac{1}{\tau^{1/2}} - \frac{1}{2\tau^{3/2}} + \frac{1 \cdot 3}{2^2 \tau^{5/2}} - \cdots\right)$$

When τ exceeds 100, or equivalently $t^* > 100$

$$\phi(\tau) \cong 2(\tau/\pi)^{1/2} \tag{21}$$

Equations (14), (17), (18) and (21) are combined to yield

$$t_{\ell 3} = (\pi/4)(\psi^* \rho' \lambda/\Delta T)^2 (R_o^2/K)$$
$$= (3\pi/4)(Q_o/q_{po})^2 \tag{22}$$

where $t_{\ell 3}$ corresponds to the droplet lifetime in this range of t^* and

$$q_{po} = 4\pi R_o^2 \psi_b k \Delta T/\alpha^{1/2} \tag{23}$$

denotes the conduction rate in the heating plate. The two asymptotic values of $\phi(\tau)$, equations (19) and (21), are superimposed on Fig. 3 as broken lines. The numbers 0.001 and 100 used as the criteria to indicate very small and large values of τ, respecitvely, are determined by comparing the solid and broken lines. It is seen that deviations of the asymptotic values from the exact $\phi(\tau)$ are confined to within 100 percents.

In the intermediate time domain of $0.001 < t^* < 100$, one can express equation (17) as $\tau^* = CY^m$, or through a rearrangement as

$$t_{\ell 2} = C(\psi^* \rho' \lambda/\Delta T)^m (R_o^2/\rho Ck)^{m-1} (R_o/U)^{2-m}$$
$$= 3^m C\, Q_o^m/(q_{po}^{2m-2} q_{bo}^{2-m}) \tag{24}$$

where $t_{\ell 3}$ is the droplet lifetime for the intermediate range of t^*. C and m are constants. Equation (24) can be reduced to equations (20) and (22) for m=1, C=1 and m=2, C=$\pi/4$, respectively. In the intermediate case, therefore, the value of m varies from 1 to 2 and C from 1 to $\pi/4$ as the value of t^* increases.

The analysis leads to a classification of the evaporation mode into three categories, (i) where the evaporation is controlled by heat transfer through the drop, (ii) where heat diffusion in the heating plate is the controlling mechanism, and (iii) the intermediate case, where both effects are of comparable importance. t^* is used to characterize the mode of evaporation. In category (i) when $t^* < 0.001$, the evaporation is independent of K, the combined property and the heating surface temperature stays constant at T_w. The droplet lifetime is completely governed by the heat transfer rate through the drop. Whereas when $t^* \geq 100$, K plays a dominant role on droplet evaporation, while the effect of the unit overall conductance through the drop U becomes negligible. In other words, the evaporation rate is con-

trolled by the temperature variation in the heating plate and therefore the surface temperature must be obtained through a distributed-parameter model. In the intermediate case, however, the evaporation is governed by both the heat diffusion rate in the heating plate and the heat transfer rate through the droplet. The relative importance of the two heat transfer rates varies with a change in t_c. In both categories (ii) and (iii), the assumption of constant surface temperature in droplet evaporation analyses would lead to a substantial error in the prediction. The error is enhanced with an increase in t_c as the role of the heat diffusion rate in the heating plate progressively becomes dominant.

It can be shown that

$$t_c = (q_{po}/q_{bo})^2, \quad t_{\ell 3}/t_c = (\pi/12)(t_{\ell 1}/t_c)^2 \tag{25}$$

In practical applications, one would first evaluate Q_o, q_{po} and q_{bo} according to their definition. $t_{\ell 1}$ and $t_{\ell 3}$ are then determined by equations (20) and (22) respectively together with t_c. In reference to equation (25), it is obvious that if the criterion for category (i) $t_{\ell 1}/t_c \leq 0.001$ is fulfilled, then that for (iii) $t_{\ell 3}/t_c \geq 100$ will not be simultaneously satisfied and vice versa. In the event neither criterion is met, then the evaporation process is in the intermediate case (iii) and Fig. 3 must be used to determine the rate and $t_{\ell 2}$.

The dimensionless parameters ψ_b/ψ_v and ψ_s/ψ_s characterize the behavior of droplet spreading on the surface. Figure 4 illustrates that the contact angle θ affects the ratios of the geometrical coefficients for a lens-shaped drop. For liquids which completely wet the solid, $\theta = 0$. In practice, a contact angle of 90° is often regarded as a sufficient criterion of non-wetting. $\theta = 90°$ corresponds to a special case for which the lens-shaped drop becomes a hemisphere. Roughness of a surface has the effect of making θ further from 90°. If the smooth material gives an angle greater than 90°, roughness increases this angle still further, making it more non-wetting. On the other hand, if θ is less than 90°, roughness decreases the angle and makes the surface more wetting. Both contact angle and surface tension decrease with an increase in the temperature. Figure 4 indicates that both ψ_s/ψ_v and ψ_b/ψ_v diminish as θ increases. However, ψ_s/ψ_v takes a minimum value at $\theta \cong 120°$. A drastic change in spreading behavior occurs for θ less than 50°.

An examination of equations (20) and (22) reveals the following: The droplet controlling evaporation mode takes place (i) when the surface is very wetting to the liquid, θ of 0° to 20° and (ii) when the liquid-solid combination has a very large value of K'/K, for example liquids on a copper surface. On the other hand, the surface controlling evaporation mechanism is observed only when the surface is very non-wetting to the liquid, θ of 160° to 180°.

Figure 5 is a plot of equation (24) for comparing the droplet lifetimes of the same liquid on various metal surfaces, using the same θ for convenience The subscript ss refers to a stainless steel (80 Cr, 20 Ni) surface. Since copper has the highest value of K, a droplet would have the shortest lifetime on it.

In order to determine the effects of physical parameters on the evaporation, equation (24) is rewritten in dimensionless form as

$$t_\ell^* = C(\psi^* \lambda^* \Delta T^*)^m (K^*)^{m-1} (U^*)^{m-2} \tag{26}$$

where $1 \leq m \leq 2$ and

$$t_\ell^* = \alpha' t_\ell / R_o^2, \quad \lambda^* = \lambda/(c'\Delta T'), \quad \Delta T^* = \Delta T'/\Delta T$$
$$K^* = K'/K, \qquad U^* = U/(k'/R_o) \tag{27}$$

$\Delta T' = T_s' - T_o$ and T_s' denotes the liquid temperature at which evaporation takes place. R_o^2/α' represents the time required for heat diffusion in a spherical drop of radius R_o. λ^* signifies the ratio of the latent heat to the sensible heat of the droplet. U^* indicates the ratio of the unit overall conductance between the heating surface and the ambient to the unit conductance through the drop. Equation (20) indicates that t_ℓ^* reduces with a decrease in ψ^*, λ^*, ΔT^* or K^* and an increase in U^*. For an easy wetting fluid characterized by θ less than 50° at room temperature, U and consequently U^* can be approximated as $(\psi_s k_a/\psi_b R_o)$ and $(\psi_s k_a/\psi_b k')$, respectively. It is seen in Fig. 4 that the value of ψ_s/ψ_b increases only slightly as θ varies from 0° to 50°. Therefore, both U and U^* remain essentially unchanged with surface temperature even though θ varies with T_w. τ^* also changes very slightly in the small θ range. However, since ψ^* depends very strongly on θ, the magnitude of Y by definition changes very significantly with θ. In dealing with the evaporation of droplets on an easy wetting solid, therefore, an accurate information on θ and its temperature dependence is essential for correlating test data.

Experimental results for droplet evaporation on a fused quartz plate [3] and an aluminum plate [4] were compared with the theory (in solid lines) in Figs. 6 and 7, respectively. The broken line in Fig. 6 corresponds to $Y = \tau^*$. It was found that equation (5-c) applies to both the conduction-controlling and lumped-parameter models, as the second term is much smaller than the first one on the RHS of equation (5-b). Since $K = 4.68 \times 10^8$ WJ/m^4-°C^2 for aluminum compared to $K = 2.12 \times 10^6$ WJ/m^4-°C^2 for quartz, liquid-aluminum combinations have much lower values of τ^* in Fig. 7 than liquid-quartz combinations in Fig. 6. Contact angles are, in general determined at 20 °C and 50% relative humidity. It is reported in references 11-14 that many liquids from an adsorbed monolayer on high free energy surfaces, i.e. high melting point solids such as silica, sapphire and most metals. As a result, a high energy surface is transformed into one with the wetting properties characteristics of a low energy surface of the same composition and packing as the monolayer. Low melting solids such as organic polymers, waxes and covalent compounds in general have low surface energy. Spreading occurs only if the liquid has a lower surface tension than the critical surface tension (at which the liquid completely wets the surface) of the adsorbed layer. Unfortunately, the critical surface tensions of most metallic surfaces and the temperature dependence of contact angles have not been investigated. In correlating data for Figs. 6 and 7, a contact angle (indicated in parenthesis) was selected in each liquid-solid combination. The choice is, of course, to some extent arbitrary but within the range appropriate to the homologous group of that combination [11-14]. For each combination, the value of Y reduces with an increase in surface temperature, resulting in a decrease in τ^*. It is common to all combinations that deviations from theoretical predictions grow as Y decreases since contact angles diminish with an increase in surface temperature, resulting in a decrease in ψ^* as shown in Fig. 4. Should the information on the contact angle-temperature relationship be available, better agreement between theory and test data is certainly warranted. It is deduced from Fig. 7 and equation (20) that the droplet lifetime on a heated aluminum plate is independent of the thermal properties of the solid material, contrary to Teshirogi's conclusion. Therefore, the evaporation mode is controlled by heat transfer through the droplet. The mode of droplet evaporation on the heated quartz surface in Fig. 6 is practically in the same category with only a slight evidence of discrepancy at high values of Y.

Conclusions and Remarks

The theoretical analysis presented herein leads to a logical classification of evaporation of droplets in direct contact with heated surfaces into three categories: (i) heat transfer through droplet controlling, (ii) plate conduction controlling, and (iii) the intermediate case where both effects are of importance. For (i) which corresponds to the case of very low contact angles or a liquid-solid combination with very large value of K^*, the evaporation rates are high and consequently the droplet lifetimes are short. The evaporation of wetting liquids on high melting solids falls into this category. In contrast, the evaporation rates are slow for (ii) which fits the case of very high contact angles. A dimensionless parameter, t^*, has been identified to characterize the evaporation mode. The lumped-parameter model may be employed to describe heat transfer conditions in the droplet. Experimental results indicates the general validity of the theoretical analysis. A handicap exists in some cases due to a lack of the information on contact angles, particularly at high temperatures. It is important to note that the present study is not applicable to the evaporation of droplets in the spheroidal state.

References

1. F. Bashforth and J.C. Adams, An Attempt to Test the Theories of Capillary Action, Cambridge University Press, Cambridge, England (1883).

2. P. Savic and G.T. Boult, The Fluid Flow Associated with the Impact of Liquid Drops with Solid Surfaces, NRC MT-26, National Research Council, Canada (May 1955).

3. Z. Tamura and Y. Tanasawa, Evaporation and Combustion of a Drop Contacting with a Hot Surface, 7th Symposium (International) on Combustion, Butterworth's Scientific Publications, London, 509 (1959).

4. N. Teshirogi, Combustion Control of Diesel Engines by Heated Surfaces (in Japanese), Doctor of Eng. Thesis, University of Tokyo, Tokyo (1975).

5. Wen-Jei Yang, Vaporization and Combustion of Liquid Drops on Heated Surfaces, in Two-Phase Transport and Reactor Safety, Vol. 1, Hemisphere Publishing Corp., Washington, D.C., 51 (1978).

6. Wen-Jei Yang, Vaporization and Combustion of Binary Liquid Drops on Heated Surfaces, Proc. 1977 Tokyo Joint Gas Turbine Congress, 77 (1977).

7. W.D. Bascom, R.L. Cottington and C.R. Singleterry, Dynamic Surface Phenomena in the Spontaneous Spreading of Oils on Solids, in Contact Angles, Wettability and Adhesion, edited by R.F. Gould, Advances in Chemistry Series, 43, Amer. Chem. Soc., Washington, D.C., 355 (1964).

8. A. Umur and P. Griffith, Mechanism of Dropwise Condensation, J. Heat Transfer, Trans. ASME, 87, 275 (1965).

9. B.B. Mikic, On Mechanism of Droplet Condensation, Int. J. Heat Mass Transfer 12, 1311 (1969).

10. H.S. Carslaw and J.C. Jaeger, Conduction of Heat in Solids, 2nd ed., Oxford University Press, London, Appendix II (1959).

11. E.F. Hare and W.A. Zisman, Autophobic Liquids and the Properties of Their Adsorbed Films, J. Phys. Chem., 59, 335 (1955).

12. H.W. Fox, E.F. Hare and W.A. Zisman, Wetting Properties of Organic Liquids on High Energy Surfaces, J. Phys. Chem. 59, 1097 (1955).

13. E.G. Shafrin and W.A. Zisman, Constitutive Relations in the Wetting of Low Energy Surfaces and the Theory of the Retraction Method of Preparing Monoloayers, J. Phys. Chem. 64, 519 (1960).

14. W.A. Zisman, Relation of the Equilibrium Contact Angle to Liquid and Solid Constitution, in: R.F. Gould (Ed.), Contact Angle, Wettability, and Adhesion, Advances in Chemistry Series 43, Amer. Chem. Soc., Washington, D.C., 1 (1964).

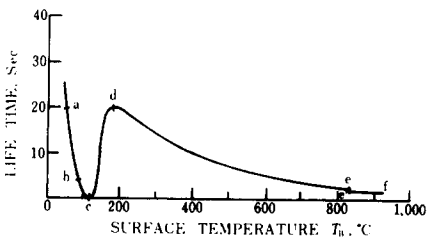

Fig. 1 Droplet lifetime curve of benzene with initial diameter of 2.14 cm

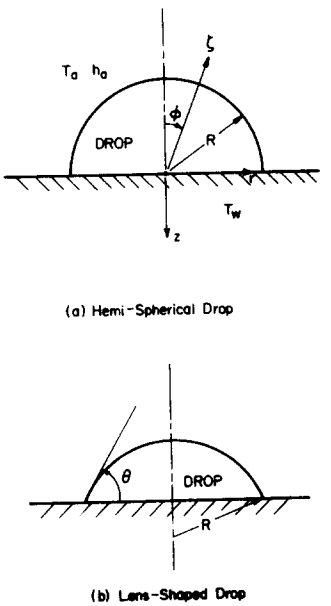

Fig. 2 Droplet geometry used in analysis

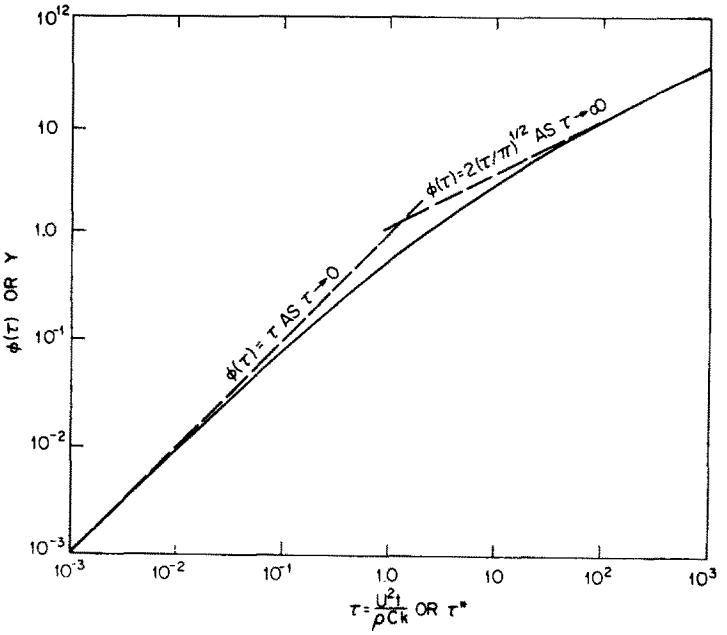

Fig. 3 $\phi(\tau)$ versus τ or Y versus τ^*

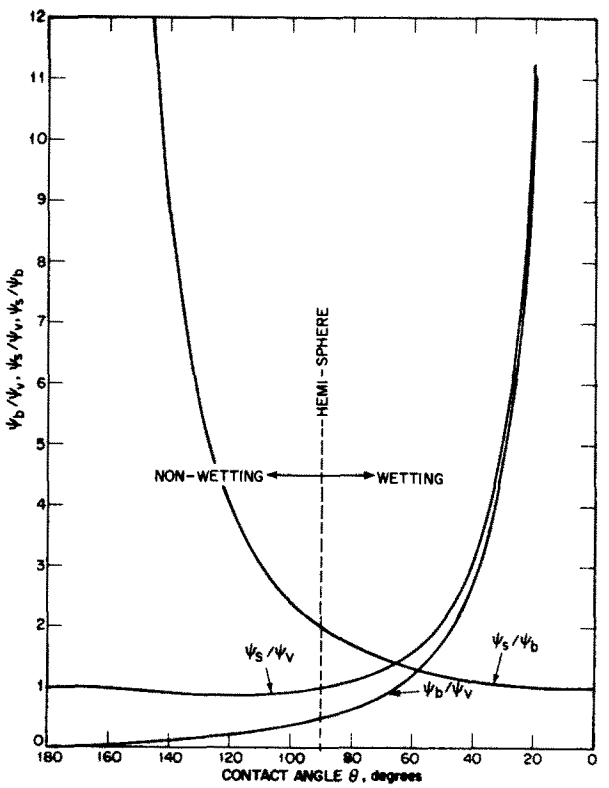

Fig. 4 ψ functions versus contact angle

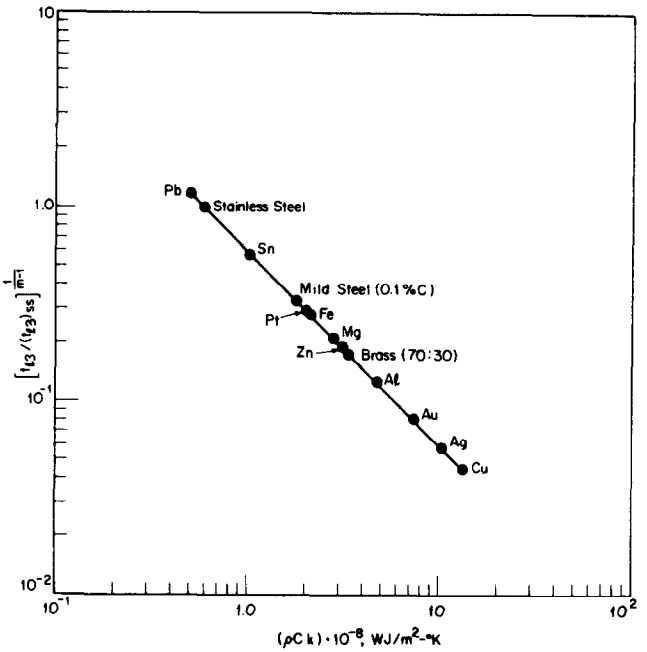

Fig. 5 Droplet lifetime $t_{\ell 3}$ on various heated metal surfaces

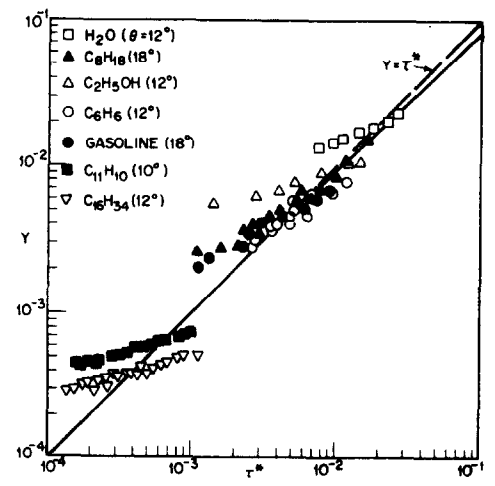

Fig. 6 Droplet evaporation on a heated quartz surface [3]

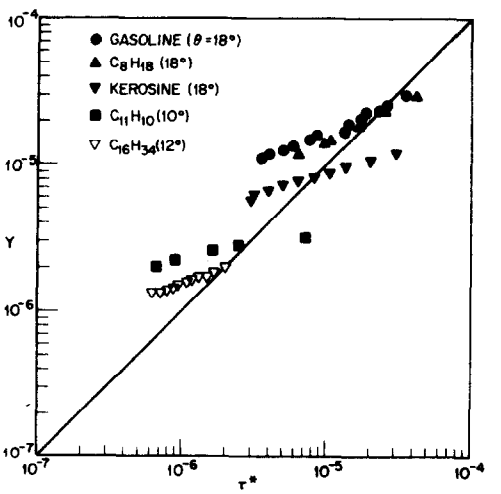

Fig. 7 Droplet evaporation on a heated aluminum surface [4]